VEÐURSTOFA ÍSLANDS

Report
03023

Kristín Martha Hákonardóttir
Tómas Jóhannesson
Felix Tiefenbacher, SLF
Martin Kern, SLF

Avalanche braking mound experiments with snow Switzerland – March 2002

VÍ-ÚR17
Reykjavík
August 2003

Contents

List of Tables

List of Figures

1 Introduction

A set of avalanche experiments has been performed to study the retarding effect of avalanche catching dams and braking mounds (short dams), using snow as the experimental material. The experiments were performed on a 34 m long and 2.5 m wide chute, situated at Weissfluhjoch on the mountainside above the town Davos in Switzerland (see Figure 1). The experimental chute was built in the late 1950's to study impact forces on obstacles. Arrays of optical velocity sensors have recently been installed in the base of the chute as well as on the sides to obtain basal velocities and vertical velocity profiles through the depth of the avalanche (Kocher, 2002). For a description of the velocity sensors and velocity data handling see Hákonardóttir and others (2001), Kocher (2002) and Tiefenbacher and Kern (submitted). The aim of the experiments was to analyse the flow over dams and over and around braking mounds and compare the results with results obtained on smaller scales, where glass particles were used as the experimental material (Hákonardóttir and others, 2001, in press). Experiments on several different scales were carried out as a part of the European Union project, Cadzie, during 1999–2002 in collaboration between the Icelandic Meteorological Office, the Department of Applied Mathematics at the University of Bristol in England and the Swiss Federal Institute for Snow and Avalanche Research (SLF).

In this study, we present results from the snow experiments on Weissfluhjoch. We describe the experimental setup (§2) and design (§3) and give a summary of the experiments that were conducted (§4). In §5, we analyse the flowing avalanche without any obstacles present on the chute and then move on to describing the flow with obstacles. We document the airborne jets which arise from the interaction (§5.1), analyse the resulting speed reduction (§5.2) and finally describe the wedges found behind the mounds after each experimental run (§5.3).

2 Experimental Setup

Section	I	II	III	IV	V
Length [m]	10.0	10.0	4.20	6.05	3.50
Inclination [°]	45	45	32	25	8

Table 1: Length and inclination of each section of the chute, see Figure 1.

A 34 m long and 2.5 m wide chute with 0.9 m high side walls was used in the experiments (Figure 1). Snow was shovelled manually into a barrell and then dumped onto the chute, behind a lock gate. During the process of loading the snow onto the chute, the chute was inclined at about 30°. The material was evenly spread out over the length of about 5 m behind the lock gate. The chute was then raised up to 45°, resulting in some buildup of snow just behind the lock gate and an approximately triangular shape of the snow when released. The

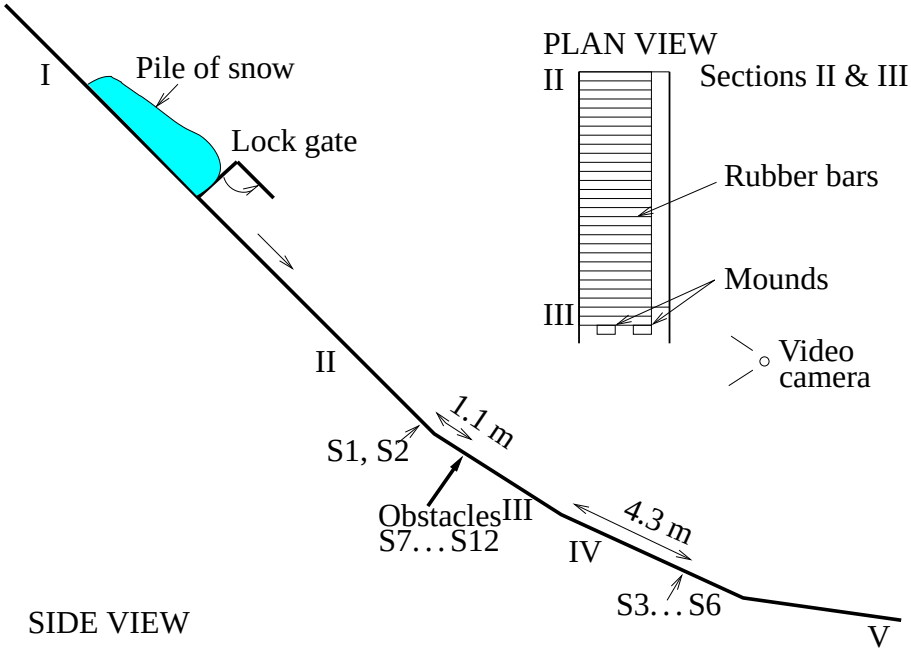

Figure 1: A schematic diagram of the experimental chute, velocity sensors are denoted by Sx.

snow flowed down the chute and then carried on down the mountainside and came to a rest on the skislope underneath (see the Appendix for photos).

In Figure 1, the chute is divided into sections I to V depending on its inclination. Section II had a slippery aluminium base and sections III, IV and V had a wooden base. Rubber bars were placed on the base of the chute above the barriers (sections II and III), to introduce turbulence into the flow. Previous test runs without rubber bars resulted in a plug type of flow. A 45 cm wide section on the right hand side of the chute (looking upstream) was not covered with rubber bars. Because of the layout of the mountainside, it was not possible to extend the run-out zone (section V) so that the avalanche would come to a rest on the chute and thus allow for using the run-out length to compare the effectiveness of different obstacle setups (as done in the previous small scale experiments). Instead velocity measurements were used for comparison.

Each experiment took at least an hour and a half to set up when five people were working together. The success of the individual experimental runs depended upon the weather, *i.e.* was subject to the snow not freezing to the experimental chute before the lock gate was opened. Section I, above the lock gate was made of aluminium and coated with a layer of paint to reduce the freezing effect. In spite of that, the experiments only ran smoothly when it was sunny and the cooling effect of the wind was not too great.

Twelve LED velocity sensors were installed along the chute to measure the flow speed (Figure 2). Sensors S1 and S2 were fixed on the base of the chute, 9.95 m down-stream from

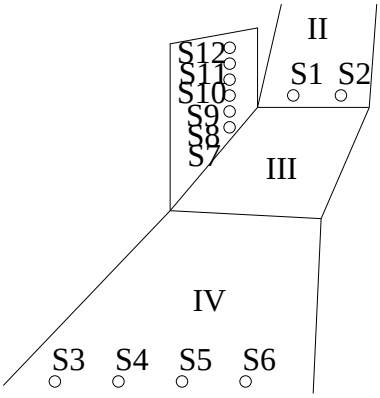

Figure 2: A schematic diagram of the layout of the velocity sensors, S1…S12, on the chute.

the lock gate. Sensors S7 to S12 formed a vertical sensor array on the sidewall, 10.6 m down stream. The lowermost sensor in the array, S7, was fixed 0.1 cm above the surface of the rubber elements on the chute. The spacing between individual sensors in the array was about 3 cm, allowing for a velocity profile measurement in the lowermost 16 cm of the avalanche. Sensors S3 to S6 were installed in the the run-out zone, 18.5 m down stream.

Experiments using obstacles consisted of two setups using mounds, *i.e.* 40 and 60 cm high mounds with a width of 60 cm, and two setups of 40 and 60 cm high dams (dams cover the whole width of the chute, while mounds only partly cover the chute), see Figure 3 and Table 2. The barriers were mounted perpendicular to the chute.

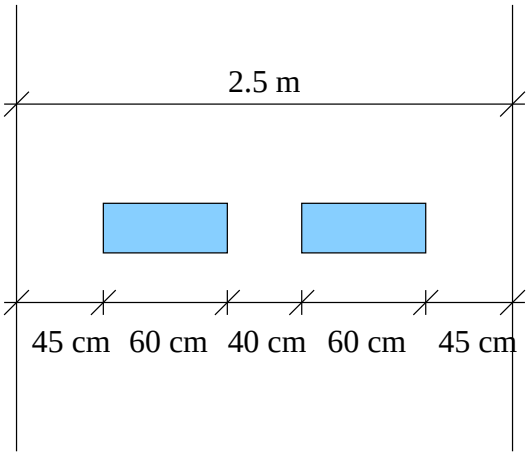

Figure 3: Planview. A schematic diagram of the mound setup.

The experiments were recorded from the right hand side (looking upstream) using a digital

Setup	H [cm]	B [cm]	#	A'	H/B
Mounds 1	40	60	2	0.48	0.67
Mounds 2	60	60	2	0.48	1.0
Dam 1	40	250	1	1.0	
Dam 2	60	250	1	1.0	

Table 2: Geometry of the different obstacle setups, H is the height of the obstacles, B is the breadth and A' is the ratio of the width of the chute covered by the mounds.

video camera, capturing 50 frames per second. Another digital camera was used for recording at the front.

3 Experimental design

The Froude number of the flow can be defined as follows

$$Fr = \frac{u}{\sqrt{g\cos(\psi)h}},$$

where u is the speed of the flow, g is the gravitational acceleration, ψ is the inclination of the chute and h is the flow depth. This dimensionless number is used to characterise free surface fluid flows.

Large, dry, natural snow avalanches often consist of a powder cloud and a denser core. The dense core can be modelled as a shallow, granular, gravity current. A typical Froude number of the dense core is on the order of 10. The design of the experiments and previous experiments on smaller scales was based on the conjecture that if the Froude numbers were on the same order of magnitude, dynamical similarity between natural snow avalanches and the smaller-scale experimental avalanches would be maintained. The Froude numbers in the snow experiments presented here were in the range 3–6 (see section Results), varying with each experimental run, depending on the condition of the snow. The wetter the snow, the slower and thicker the avalanche. These were the highest Froude numbers that the experimental setup allowed for, and they were somewhat lower than would have been preferable.

A corresponding obstacle Froude number can be defined as

$$Fr = \frac{u}{\sqrt{g\cos(\psi)H}},$$

where H denotes the height of the obstacles. The snow experiments yielded obstacle Froude numbers in the range 2–4, these were in the same range as in the previous experiments on smaller scales.

4 Diary

The experiments were performed in a 3 day wake of sunny and calm weather after the first real snow of the season. Experiments where no obstacles were present on the chute were termed control experiments. The different obstacle setups are defined in Table 2. Table 3 gives an overview of the experiments that were carried out.

	Setup	Morning	Afternoon	Comments
11.3. Exp. 1	Control 1	X		$\sim$ 8 m^3 of snow were released
Exp. 2	Control 2		X	$\sim$ 5 m^3 of snow were released
12.3. Exp. 3	Mounds 1	X		
Exp. 4	Mounds 1	X		
Exp. 5	Dam 1		X	Only half of the snow was released
13.3. Exp. 6	Dam 1	X		The snow was released in 2 goes
Exp. 7	Dam 1	X		
Exp. 8	Dam 2	X		A small section of the dam broke
Exp. 9	Mounds 2		X	

Table 3: A list of the experiments that were carried out during the three day experimental period.

About 5 m^3 of snow were released in the experimental runs with obstacles. A release of 5 m^3 of snow resulted in a lower flow height than when 8 m^3 were released and reduced the setup time considerably (less shovelling!). The specific weight of the snow in the experiments was estimated to be in the range 300–400 kgm^{-3} leading to a release of 1.5 to 2 tons of snow in each run. In general, the snow became wetter as the day advanced, starting with dry snow in the morning. The wetness of the snow probably affected the flow depth and the flow speed of the avalanches (the flow becoming deeper and slower when wetter).

In experiment 8, a 45 cm long section at the bottom right hand side (looking upstream) of the dam broke, otherwise the run was successful. This is the area where no rubber bars were present on the base of the chute. It was apparent from the video analysis that the part of the avalanche near this side of the chute was flowing at a higher speed ($\sim$1–2 ms^{-1}) than the snow on the rubber covered part of the chute. The velocity sensors were all mounted on the other side of the chute within the area covered by the rubber elements. The higher flow speed close to the right hand side of the chute should therefore not have disturbed the velocity measurements.

Experiments 1, 2, 3, 4, 7, 8 and 9 were considered successful and will be analysed in the following sections.

5 Results

The snow used in the experiments varied from being dry to being wet and it contained fine snow along with snow lumps with a diameter up to 10 cm. When the snow was released it extended 5 to 6 meters behind the lock gate. After the release the avalanche spread longitudinally on the chute, and had a length of about 8 meters before reaching the mounds. A head and a tail were detected from the video recordings of the control runs. The head was about 10 cm higher than the snow immediately following. The bulk of the avalanche had a thickness of 30 ± 10 cm and a flow speed of 7 ± 1 ms^{-1} just in front of the obstacles, depending on the condition of the snow in each experiment. Flow speeds were recorded during each experiment, see Table 4, but the flow thickness was only well determined for the two control runs, from video recordings of the flows. Consequently, considerable uncertainty is attached to the flow depth. In general, the wetter avalanches may be expected to be thicker than the dry ones. Technical problems prevented the derivation of consistent velocity estimates from the signal from sensors S3...S6 for Exp. 8 and 9 (the 60 cm mounds and the 60 cm dam).

Setup	S1, S2 [ms^{-1}]	S8...S12 [ms^{-1}]	S3...S6 [ms^{-1}]
Exp. 1: C1	7.75 ± 1.0	7.75 ± 0.25	10.25 ± 0.25
Exp. 2: C2	6.5 ± 0.5	6.5 ± 0.5	9.5 ± 1.0
Exp. 3: M1	8 ± 1	7 ± 0.5	8 ± 1
Exp. 4: M1	(7.25)	7.25 ± 0.75	8 ± 0.5
Exp. 7: D1	7.5 ± 1	7.5 ± 1.5	7 ± 0.5
Exp. 8: D2	(7.5)	7.5 ± 0.25	—
Exp. 9: M2	7.5 ± 1	7.5 ± 0.5	—

Table 4: Velocity recordings at different sensors, Sx, along the chute after cleaning of the velocity signal had taken place. The values in parentheses were not determined from the signals, since the signal processing did not produce useful velocities, the velocities at S8...S12 were therefore used instead. Sensors S1, S2 and S3...S6 were located at the base of the chute and velocities recorded by these sensors might therefore be slightly lower than the velocity of the centre of the avalanche. Sensors S8...S12 were mounted on the side of the chute and might therefore also record slightly lower velocities than at the centre of the avalanche. Velocity measurements from sensors S3...S6 for Exp. 8 and 9 (the 60 cm mounds and the 60 cm dam) are unavailable due to technical problems.

The head of the control avalanche travelled with the maximum flow speed which was then maintained for about 1 s and so was the depth of the flow after the head had passed (video analysis). The flow height and speed decreased towards the tail of the avalanche, and near the end, only separated snow lumps slid down the chute. Velocity profiles through the avalanche showed that the flow could be split into two parts based on the order of magnitude of the velocity gradient in each part. Between sensors S8 and S12, the velocity gradient was on the

order of 10 s^{-1}. Near the bottom, between sensors S7 and S8 (vertical spacing of 3.7 cm), the mean velocity gradient was on the order of 100 s^{-1}, which is an order of magnitude higher than in the snow above. This implies a strong shear deformation at the contact of the snow and the underlying rough chute surface. It was also found that the velocity at the bottom of the chute varies strongly, but is non-zero for all experiments. See Kocher (2002) for a more detailed discussion.

Experiments with barriers resulted in jets launched from the top of the obstacles (Figure 4). The duration of each avalanche was short (only about 1 s before the avalanche started to slow down considerably), so the jets were essentially only a first front taking off from the top of the barriers. A steady jet, as was observed in the smaller scale experiments, did not form.

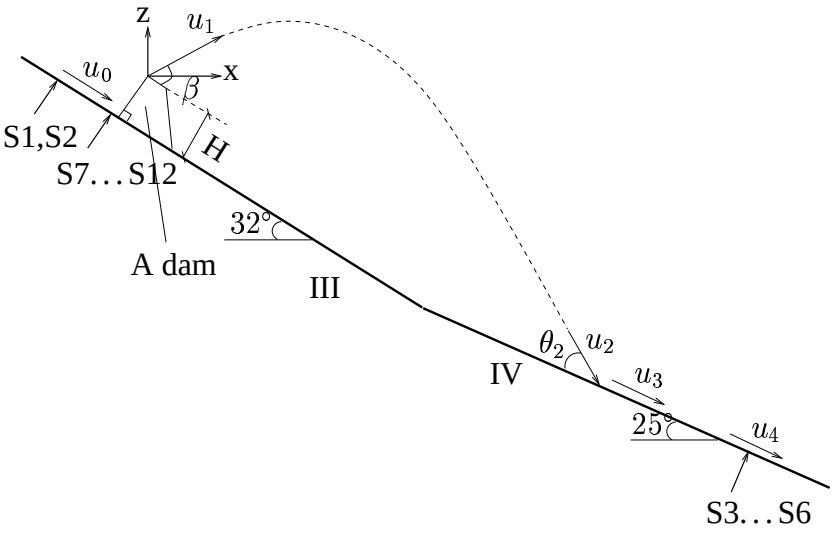

Figure 4: A schematic diagram of a jet jumping over a dam on the chute, side view. The speeds, u_0, u_1, u_2, u_3 and u_4 defined, along with the throw angle, β, the height of the dam, H, and the angle θ_2 between the lower end of the jet and the chute.

5.1 Jet trajectories

The trajectories taken by the first front of the jets were studied from video recordings for flows over the two dams by tracking the first front of the flow. By treating the jet as a two-dimensional ballistic projectile, without air resistance, it is possible to write down a formula for the jet trajectory as a function of the throw angle, β, and the launch speed, u_1;

$$z = x \tan(\beta - 32^\circ) - \frac{1}{2}\frac{gx^2}{u_1^2}\sec^2(\beta - 32^\circ).$$

Throw angles and launch speeds were calculated indirectly by fitting parabolas to the observed jet trajectories through least square fits (Figure 5).

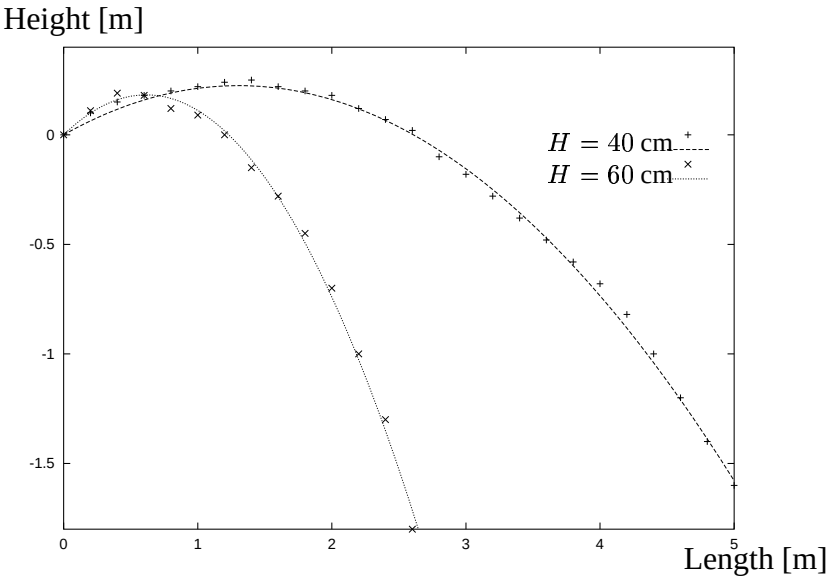

Figure 5: Jet trajectories for the two dams. The points show the observed trajectories and the lines denote the corresponding fitted parabolas. The length and height is measured from the top of the dam horizontally and vertically.

The trajectory for the 40 cm high dam was not as well defined as for the 60 cm high dam. That might be caused by the difference in the wetness of the snow (the snow being considerably wetter in the experiment with the higher dam). It was thus possible to fit a number of parabolas to the observed trajectory of the avalanche, resulting in different values of throw speeds and angles. In order to obtain a trajectory for the 40 cm high dam, it was necessary to choose a plausible trajectory that corresponded to the horizontal front velocity of the jet as measured from the video recording. The observed trajectory for the 60 cm high dam was much better defined and the obtained throw speed (calculated from the parabola fitted to the trajectory) was in agreement with the horizontal speed measured from the video recording (see Table 5). There is no suggestion that air resistance is affecting the jets, *i.e.* the shape of

H [cm]	u_0 [ms^{-1}]	β [$^\circ$]	u_1 [ms^{-1}]	θ_2 [$^\circ$]	u_2 [ms^{-1}]
40	7.5$\pm$1.5	51	6.1$\pm$0.4	41	14
60	7.5$\pm$0.25	63	3.7$\pm$0.1	50	11.5

Table 5: Incoming speeds, u_0, measured at sensors S8...S12, launch speeds, u_1, and throw angles, β, for the jets over the 40 and 60 cm high dams. The accuracy range was obtained by comparing the horizontal part of the launch speed, u_1, to the horizontal speed of the first front of the jet, measured from the video recording. The speed, u_2 and angle θ_2 were calculated from the jet trajectories, using β and u_1.

the jet is well approximated by a parabola and the velocity in the x-direction, found from the video analysis, seems to be constant.

The inviscid irrotational flow over a dam has been studied theoretically when the effect of gravity is negligible (Yih, 1979). Using free-streamline theory and conformal mappings of the complex potential, it is possible to derive an expression for the throw angle of the jet as a function of the height of the dam relative to the depth of the flow and the inclination of the upstream dam face, α (here, $\alpha = \pi/2$). For the jet defined by Figure 4, Yih derived the following expression for the height of the dam relative to the depth of the incoming stream.

$$\begin{aligned}\frac{H}{h} &= \mathrm{Im}\Bigg(\frac{1}{\pi}\sum_{r=0}^{m-1}\Big\{\exp\left(-i(2r\alpha+\beta)\right)\ln\left[1-\exp\frac{i(\alpha-2r\alpha-\beta)}{n}\right] \\ &\quad -\exp\left(-i(2r\alpha-\beta)\right)\ln\left[1-\exp\frac{i(\alpha-2r\alpha+\beta)}{n}\right] \\ &\quad +2\exp(-i2r\alpha)\ln\left[1-\exp\frac{i(\alpha-2r\alpha)}{n}\right]\Big\}\Bigg),\end{aligned}$$

where $\alpha = \pi n/m$. This expression provides an implicit relationship between the height of the dam relative to the flow depth and the throw angle.

Figure 6 shows the throw angle plotted against the non-dimensional dam height for the two dams ('Snow experiment') and also results from previous experiments on smaller scales ('Series i, ii and iii') where glass particles were used along with the theoretical prediction for a fluid jet ('Theory') and results from an experiment with fluid jets ('Fluid experiment'). The snow avalanches seem to be following the same trend as the theory predicts, *i.e.* the current gets deflected at a steeper angle as the dams become higher. The experimental results are close to the theoretical curve for small values of the non-dimensional dam height. As H/h increases, the throw angle approaches an angle that is 10–20° lower than the angle between the experimental chute and the upstream dam face, *i.e.* $\alpha = 90°$, that the theory predicts.

5.2 Speed reduction

The energy dissipation involved in the impact of the avalanche and the obstacles can be observed by plotting the ratio of the incoming speed and the launch velocity. Energy balance, leads to the following formula for the relative velocity reduction, D, in the impact:

$$D = \frac{u_1}{\sqrt{u_0^2 - 2gH\cos 32°}}.$$

This ratio is plotted in Figure 7 for the 40 and 60 cm high dams. It should be noted that the incoming speed, u_0, is measured at the side of the chute (sensors S8...S11) and could therefore be slightly lower than the speed at the centre of the avalanche (drag at the sides). The launch speed, u_1, is calculated from the observed trajectories and represents the speed of

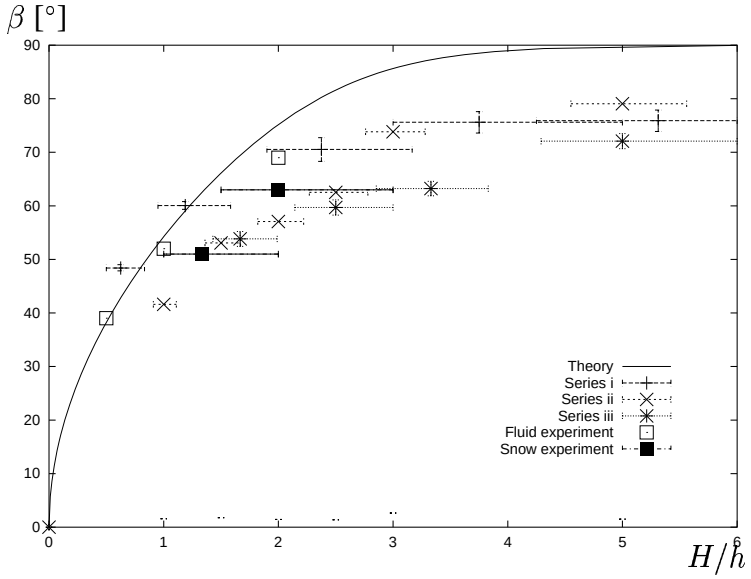

Figure 6: The throw angle, β, of a jet plotted against the non-dimensional dam height, H/h, for dams with an upstream face inclined at $\alpha = 90°$ to the experimental chute. 'Series i, ii, iii' are experimental results on smaller scales where glass beads were used to form a supercritical granular flow. The solid line denotes the theory. Results from experiments using fluids from Yih (1979) are also shown.

the centre of the avalanche. The graph suggests that there is considerable energy dissipation involved in the impact of the snow with the dams. The high uncertainty in the speed associated with the lower dam makes it hard to distinguish between the effectiveness of the two dams.

The flow speed in the control experiments (no obstacles present on the chute) is denoted by u_{cont}. It is possible to compare the speed at sensors S3...S6 for different obstacle setups to the control runs and thus compare the effectiveness of the different mound and dam setups after the jet had landed. Since the flow speed varied in each experiment (see Table 4), it was not obvious how to compare the runs with obstacles to the control runs. There exist measurements for two control runs. By using a linear interpolation of the control run flow speed at sensors S1 and S2 and also at S3...S6, a prediction was obtained for the flow speed without obstacles at sensors S3...S6 for a certain flow speed measured at S1 and S2 (or S8...S12), see Table 6.

The relative speed reduction, u_4/u_{cont}, at S3...S6 is plotted in Figure 8 for the experiments with the 40 cm high dam and mounds. It shows that the obstacles reduce the speed at S3...S6 considerably. The velocity u_4 is not available for the 60 cm high obstacles and the relative speed reduction can, therefore, not be plotted for that case.

The obstacles in the snow experiments were situated in a slope of $32°$ and the jets landed again on a $25°$ slope. In this geometry, the jets of snow accelerate on the way down and reach a flow speed that is higher than the launch speed, u_1, when they land back on the chute, see u_2 in Table 5. Figure 8 and Tables 5 and 6 show that a considerable energy dissipation takes

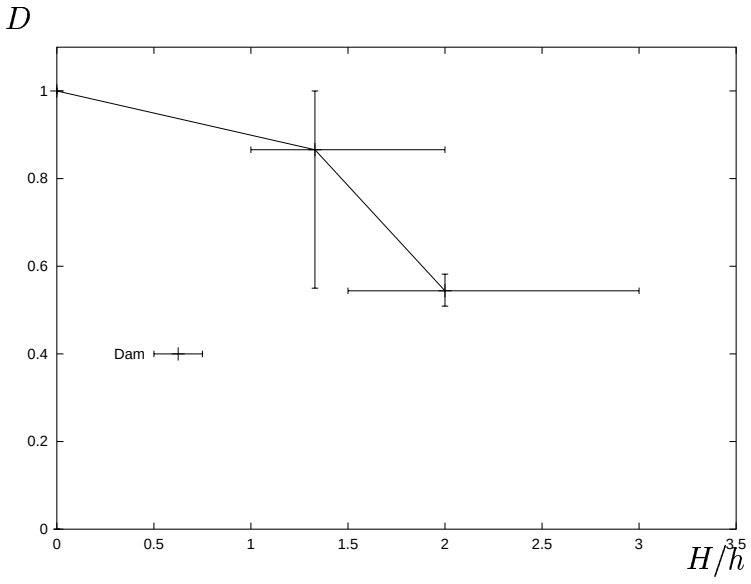

Figure 7: Relative velocity reduction, $D = u_1/\sqrt{u_0^2 - 2gH\cos 32^\circ}$, plotted against non-dimensional dam height, H/h, for the two dams.

Setup	u_0 [ms^{-1}]	u_{cont} [ms^{-1}]	u_4 [ms^{-1}]
Exp. 1: C1	7.75±0.25	10.25±0.25	10.25±0.25
Exp. 2: C2	6.5±0.5	9.5±1	9.5±1
Exp. 3: M1	7.0±0.5	10	8±1.0
Exp. 4: M1	7.25±0.75	10	8±0.5
Exp. 7: D1	7.5±1	10	7±0.5
Exp. 8: D2	7.5±0.25	10	—
Exp. 9: M2	7.5±1	10	—

Table 6: Speed measurements used to create Figure 8. The control velocity, u_{cont}, at the location of sensors S3…S6, was calculated for Exp. 3 to 9, by a linear interpolation of the measured speeds in the control runs (Exp. 1 and 2). Velocity measurements from sensors S3…S6 for Exp. 8 and 9 (the 60 cm mounds and the 60 cm dam) are unavailable due to technical problems. Therefore, the relative velocity reduction cannot be estimated for the higher obstacles.

place in the landing on the chute (compare u_2 and u_4 for the 40 cm dam in Tables 5 and 6). This energy dissipation may be expected to depend on the angle, θ_2, between the jetstream and the chute as the jet lands.

For setups with mounds, the flow becomes more complicated since the snow is deflected sideways over a mound, as well as directly over it, and subsequently interacts with the jet

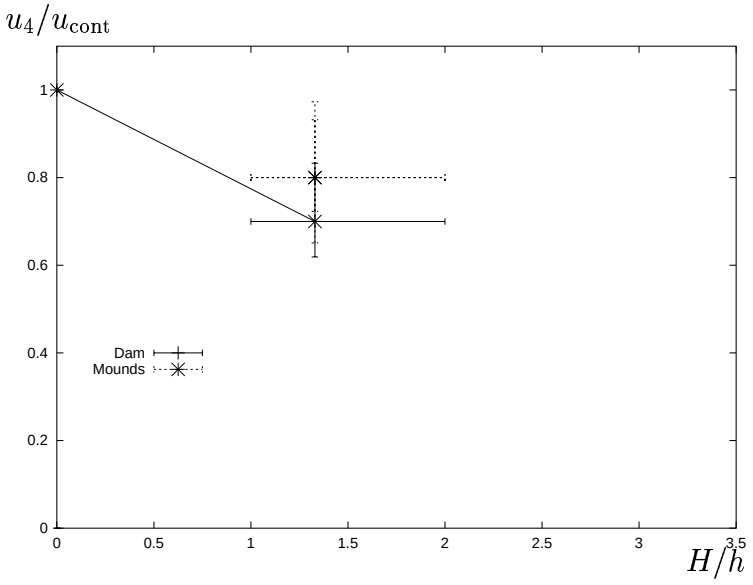

Figure 8: Relative velocity reduction, u_4/u_{cont}, at S3...S6 plotted against non-dimensional dam height, H/h, for the 40 cm high dam and mounds.

launched from the other mound. This interaction of adjacent jetstreams may be expected to introduce additional energy dissipation. It is worth bearing in mind that there were only two mounds on the chute in the snow experiments. The energy dissipation (if any) associated with the interaction of different jet streams, might play a larger role when more mounds are present.

5.3 Wedge

After each run wedges were found behind the mounds, see the last Figure in the Appendix. The video recordings showed considerable lateral deflection of the jets of snow during the impact with the mounds, as if the avalanche was deflected parallel to the planes of the side faces of the wedge. If the wedge is built up and maintained by the main flow of the avalanche, its geometry determines the way in which the avalanche is deflected over and around the mound. The wedge might nevertheless be partly built up by the tail of the flow, flowing at lower speeds than the bulk of the avalanche.

Similar wedges were seen in the small scale laboratory experiments and have also been observed behind rocks after pyroclastic flows.

6 Conclusions

The main conclusion of this set of experiments is that similar flow features are observed in the interaction of the snow avalanches and the obstacles as were previously observed in

experiments on much smaller scales using other materials. Jets of snow were launched from the top of the obstacles and subsequently landed back on the chute farther down. The Froude number of the experiments was somewhat lower than believed to be appropriate for large natural snow avalanches, *i.e.* 3–6 instead of 10, and the thickness of the avalanche and the flow speed varied between the experiments depending on the wetness of the snow. In spite of the Froude number being lower than preferred and the ever changing snow conditions, the flow behaviour around the obstacles was similar to what was found in the smaller scale experiments. This suggests that the behaviour of the supercritical flow around the obstacles is not strongly dependent on the Froude number, but is governed by the large-scale properties of the flowing avalanche (*i.e.* flow depth and speed) rather than micro-scale properties of the granular current.

The experiments suggest the following behaviour of an avalanche hitting a catching dam and a row of braking mounds:

Dam. The snow hits the dam and is subsequently launched from the top of the dam and forms a jet that lands farther down on the chute. The jet can be treated as a two-dimensional ballistic projectile without air resistance. As the dam becomes higher, more energy is lost in the impact and the trajectory taken by the jet becomes steeper. Energy is dissipated in the impact with the dam and also in the landing of the jet on the chute.

Braking mounds. The snow is deflected over and around the mounds and an interaction between jets launched from individual mounds takes place. The wider the mounds become, compared to their height, the less significant/effective the lateral deflection becomes and the mounds are more like dams (a result from the small scale experiments). Energy dissipation takes place in the impact of the avalanche with the mounds and most likely also in the interaction of jets from adjacent mounds. Energy dissipation, furthermore, takes place in the landing of the jets on the chute and the subsequent mixing with snow flowing in between the mounds.

Comparison of velocity measurements at sensors S3. . . S6 (see Figure 8) with and without obstacles shows that dams and mounds with a height two to three times the flow depth and a steep upstream face can reduce the kinetic energy of the flow downstream of the landing point of the jet by on the order of 30–40%. This dissipation introduced by the obstacles is on a similar order of magnitude of as may be inferred from observations of run-out reduction in experiments at smaller scales with other materials (Hákonardóttir and others, 2001, in press).

Velocity measurements through the depth of the avalanche revealed that the lowermost part of the avalanche was flowing at a considerably lower velocity than the main part, resulting in a velocity gradient that was an order of magnitude higher close to the base than through the rest of the avalanche. This suggests that there is a highly active shear layer close to the base of the avalanche, on top of which the bulk of the avalanche is flowing, much like a plug flow.

Further experiments are planned on the chute on Weissfluhjoch for next winter 2002–2003. The release mechanism of the chute will be improved and additional force measurements will

take place. The velocity data handling has also been improved as described by McElwaine and Tiefenbacher (in press), reducing uncertainties in the speed measurements.

7 Acknowledgements

The experiments described in the paper were carried out with the support from the European Commission (the research project Cadzie, grant EVG1-1999-00009) and the Icelandic Avalanche Fund. KMH acknowledges the financial support of the University of Bristol and the Icelandic Research Council. Thanks are due to Andy Hogg, Thomas Kocher, Hanna Rattay, Barbara Thurnbull, Christian Simion and Florian Michel who took part in the experiments.

8 References

Hákonardóttir, K. M., A. J. Hogg, T. Jóhannesson, and G. G. Tómasson. In press. A laboratory study of the retarding effects of braking mounds on snow avalanches. *Journal of Glaciology*.

Hákonardóttir, K. M., T. Jóhannesson, F. Tiefenbacher, and M. Kern. 2001. *A laboratory study of the retarding effect of braking mounds in 3, 6 and 9 m long chutes.* Reykjavík, Icelandic Meteorological Office, Report No. 01007.

Kocher, T. 2002. Measurements on the internal avalanche velocity and the effect of obstacles in the avalanche flow path. Zürich, Swiss Federal Institute of Technology, Department of Earth Sciences. (Diploma Thesis).

McElwaine, J. N., and F. Tiefenbacher. In press. Calculating internal avalanche velocities from correlation with error analysis. *Surveys in Geophysics*.

Tiefenbacher, F. and M. Kern. Submitted. Experimental devices to determine snow avalanche basal friction and velocity profiles. Submitted to *Cold Reg. Sci. Tech.*

Yih, C.-S. 1979. *Fluid Mechanics*. USA, West River Press.

A Appendix: Photographs from the experiments

The photographs display respectively, from the upper left hand corner to the bottom right:

- The experimental chute and the SLF building on Weissfluhjoch.
- Shovelling into the barrell. Four barrells of snow were used in each experiment with obstacles.
- The snow being transported onto the chute.
- Reshovelling and levelling of the snow on the chute, behind the lock gate.
- The experimental chute has been raised up to $45°$ and a control run is about to take place.
- The lock gate has been lifted and the snow flows down.
- The velocity sensor array, S7...S12.
- Mound setup 2, 60 cm wide and 60 cm high mounds.
- An avalanche jumping over the mounds.
- A wedge left behind a mound.